Water molecule reorganization in cytochrome *c* oxidase revealed by FTIR spectroscopy

Amandine Maréchal and Peter R. Rich[1]

Glynn Laboratory of Bioenergetics, Institute of Structural and Molecular Biology, University College London, Gower Street, London WC1E 6BT, United Kingdom

Edited by Harry B. Gray, California Institute of Technology, Pasadena, CA, and approved April 4, 2011 (received for review January 4, 2011)

Although internal electron transfer and oxygen reduction chemistry in cytochrome *c* oxidase are fairly well understood, the associated groups and pathways that couple these processes to gated proton translocation across the membrane remain unclear. Several possible pathways have been identified from crystallographic structural models; these involve hydrophilic residues in combination with structured waters that might reorganize to form transient proton transfer pathways during the catalytic cycle. To date, however, comparisons of atomic structures of different oxidases in different redox or ligation states have not provided a consistent answer as to which pathways are operative or the details of their dynamic changes during catalysis. In order to provide an experimental means to address this issue, FTIR spectroscopy in the 3,560–3,800 cm^{-1} range has been used to detect weakly H-bonded water molecules in bovine cytochrome *c* oxidase that might change during catalysis. Full redox spectra exhibited at least four signals at 3,674(+), 3,638(+), 3,620(–), and 3,607(+) cm^{-1}. A more complex set of signals was observed in spectra of photolysis of the ferrous-CO compound, a reaction that mimics the catalytic oxygen binding step, and their D_2O and $H_2{}^{18}O$ sensitivities confirmed that they arose from water molecule rearrangements. Fitting with Gaussian components indicated the involvement of up to eight waters in the photolysis transition. Similar signals were also observed in photolysis spectra of the ferrous-CO compound of bacterial C*c*O from *Paracoccus denitrificans*. Such water changes are discussed in relation to roles in hydrophilic channels and proton/electron coupling mechanism.

energy coupling | mitochondria | respiratory chain | complex IV

Mitochondrial cytochrome *c* oxidase (C*c*O) catalyses electron transfer from cytochrome *c* to molecular oxygen, conserving the released energy as coupled transmembrane proton transfers. It is a member of a homologous "superfamily" of oxidases that includes diverse bacterial forms; all types in the C*c*O subgroup contain a common "catalytic core" of subunits I, II, and III with equivalent metal centers of Cu_A, heme *a*. and a binuclear center (BNC) that is formed from heme a_3 and Cu_B (1, 2). Structures of bovine mitochondrial (3, 4) and various bacterial (5–7) C*c*Os have been solved at atomic resolution and show common details in the binuclear heme a_3/Cu_B catalytic site, other cofactors, key amino acids, and several unusual structural features. These structural data, coupled with a substantial body of biophysical and spectroscopic studies, have provided detailed information on internal electron transfer and the chemical catalytic cycle of oxygen reduction.

Crucially, however, these structural data have not provided a single picture for all forms of C*c*O of the pathway(s) for coupled proton transfer and, therefore, the interplay between electron transfer/oxygen chemistry and the intraprotein proton transfer reactions that result in proton-motive action. Crystal structures of bacterial forms of C*c*O reveal two possible proton transfer pathways in subunit I, termed the "D" and "K" pathways (5). The D pathway leads from the negative aqueous phase toward a functionally crucial glutamic acid (bovine E242; *Paracoccus denitrificans* E278; *Rhodobacter sphaeroides* E286) that is close to both hemes *a* and a_3, whereas the K pathway leads from the negative aqueous phase toward the BNC (5). A wide range of studies, in particular with mutants of bacterial C*c*O, have suggested that the K pathway delivers the first, and possibly the second, proton to the BNC for water formation, whereas the D pathway provides a common pathway both for the additional two to three protons required for water formation in the BNC and for all four of the translocated protons (8, 9). However, a number of key aspects of this model remain unresolved. First, in most structures there is no clear proton connectivity between the end of the D channel and E242 or from E242 to the BNC or the subsequent proton translocation path. Related to this is the question of how protons on E242 are correctly gated between the proton translocation path and the BNC. A further major challenge has arisen from structural studies of bovine mitochondrial C*c*O where a quite different redox- and ligand-sensitive "H" pathway (4, 10) has been suggested to provide the proton translocation path. Mutations in this H pathway in bovine C*c*O appear to uncouple proton translocation (10). An equivalent H pathway is present but not continuous in bacterial C*c*Os, but mutations in this region show no effect on coupling (11, 12). However, no structural changes have been seen in the bacterial D channel (7, 13), and to date only changes in the K and H pathways have been discerned in structures of the *Rb. sphaeroides* C*c*O (7).

Water molecules are found within all three hydrophilic channels, though the H-bonded networks that they form with hydrophilic amino acids are incomplete. Instead, as is necessary to prevent uncoupling, dynamic changes of structured waters and associated amino acids are envisaged (4, 14). Indeed, molecular dynamic simulations suggest that additional internal waters might be present in protonic "gaps" in crystallographic data and that transient water reorganization is feasible during catalysis that could make/break specific proton pathways (14). FTIR work on bacteriorhodopsin (15, 16) and photosystem II (17) has shown that structural changes of water molecules can be monitored if they are either weakly or strongly hydrogen-bonded or occur as protonated clusters (16). In the case of weakly H-bonded waters (or those with a "dangling" bond), the OH stretch bands are narrowed and the ν_{as} components can upshift into the 3,500–3,800 cm^{-1} range where they can be detected because they are outside the strong 3,200–3,500 cm^{-1} absorption envelope of liquid water (18, 19). These and other types of structured waters have been observed by time-resolved FTIR methods to play key roles during the protonmotive photocycle of bacteriorhodopsin (16). Here we show that weakly H-bonded water molecules are also present in C*c*O and that their properties are influenced by redox and ligand state changes.

Author contributions: A.M. and P.R.R. designed research; A.M. performed research; A.M. and P.R.R. analyzed data; and A.M. and P.R.R. wrote the paper.

The authors declare no conflict of interest.

This article is a PNAS Direct Submission.

[1]To whom correspondence should be addressed. E-mail: prr@ucl.ac.uk.

This article contains supporting information online at www.pnas.org/lookup/suppl/doi:10.1073/pnas.1019419108/-/DCSupplemental.

Results and Discussion

Redox-Linked Water Molecule Changes. Fig. 1 shows the electrochemically induced reduced *minus* oxidized FTIR difference spectrum of bovine C*c*O at pH 8.5. Data in the 1,800–1,400 cm^{-1} range (Fig. 1*B*) are similar to published spectra (20, 21). The troughs at 1,749 and 1,736 cm^{-1} arise from two protonated carboxylic amino acids. Similar, but simpler, changes occur in the same frequency range in redox spectra of C*c*O from *P. denitrificans*, *Rb. sphaeroides*, and *Escherichia coli* (22–24) and have been assigned to their E242 equivalent (E278, E286, and E286, respectively). The bovine C*c*O 1,749 cm^{-1} component, which also appears in the ferrous state of bovine C*c*O after CO photolysis, most likely also arises from E242, which undergoes a downshift because of increased H bonding to its immediate environment (25). The 1,736 cm^{-1} band is from a different residue, possibly D51 (26) and appears to arise from an intensity decrease, caused either by deprotonation or by a decreased bond polarity. The high-frequency IR range of the same redox spectrum of bovine C*c*O (Fig. 1*A*) has bands at 3,674(+) and 3,638(+), 3,620(−) and 3,607(+) cm^{-1}. These bands, which are roughly 8 times weaker than the signals in the carboxyl region, are typical for weakly H-bonded water molecules (15). This region of the redox difference IR spectra of C*c*O from *P. denitrificans* has been reported (27). In this case, a band at 3,610 cm^{-1} appeared in the reduced state and was interpreted as possibly a water formed on reduction within the BNC. Our data in Fig. 1*B* have been simulated with three positive and one negative Gaussian components, which must arise from at least three species appearing or undergoing bandshifts. However, the fit indicates that additional, weaker signals are also present in this region, though these cannot be assigned quantitatively with confidence at the current signal/noise level. The dominant 3,620(−)/3,607(+) cm^{-1} component may be related to the 3610 cm^{-1} band reported in C*c*O from *P. denitrificans* (27), but in our case appears to be a shift, indicating a water molecule that is present in both oxidized and reduced states.

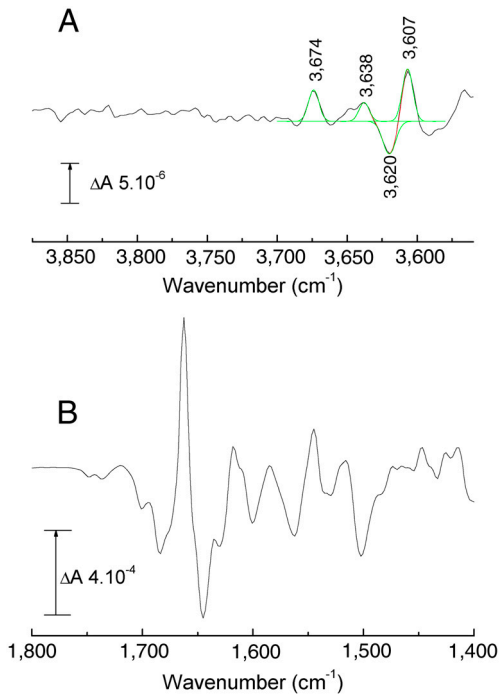

Fig. 1. Electrochemically induced reduced minus oxidized ATR-FTIR difference spectra of bovine C*c*O. (*A*) High-frequency (3,875–3,560 cm^{-1}) region (black). Data were fitted with a combination of four Gaussian components, each of 7–9 cm^{-1} FWHM (red trace; individual Gaussians shown in green); (*B*) 1,800–1,400 cm^{-1} region.

Ligand-Linked Water Molecule Changes. CO photolysis/rebinding to fully reduced bovine C*c*O is particularly convenient for FTIR investigations of ligand-induced changes as the ferrous-CO complex can be repetitively photodissociated and recombined. CO-photolysis spectra of bovine C*c*O and other homologues have been well characterized in the 2,200–1,000 cm^{-1} range (21, 28, 29). Fig. 2*A* shows CO-photolysis spectra of bovine C*c*O in the high-frequency range at pH 8.5 in a standard $H_2{}^{16}O$ buffer (top trace). A complex pattern of band changes is evident with frequencies ranging from 3,560 to 3,680 cm^{-1} and intensities 4–5 times lower than that of the 1,749/1,741 cm^{-1} carboxyl group bandshift (Fig. S1).

The same CO-photolysis difference spectrum was recorded in D_2O media (Fig. 2*A*, middle trace). The spectrum shown was scaled to that in $H_2{}^{16}O$ based on their intensities of the CO stretching mode at 1,963 cm^{-1} (Fig. S1*A*). This resulted in the disappearance of all major features in the 3,560–3,700 cm^{-1} range and lends weight to their assignment to water OH stretches since H/D exchange should cause an approximate 900 cm^{-1} downshift of their frequencies (30). To confirm this assignment, the same photolysis spectrum was recorded in $H_2{}^{18}O$ media. In this case, all bands (apart from one of the positive bands in the 3,645–3,630 cm^{-1} region) were still evident but downshifted by 6–18 cm^{-1} (Fig. 2*A*, lower trace, and Table S1), close to the 14 cm^{-1} downshift observed for the OH ν_{as} band in model water studies (30). These isotope effects demonstrate definitively that

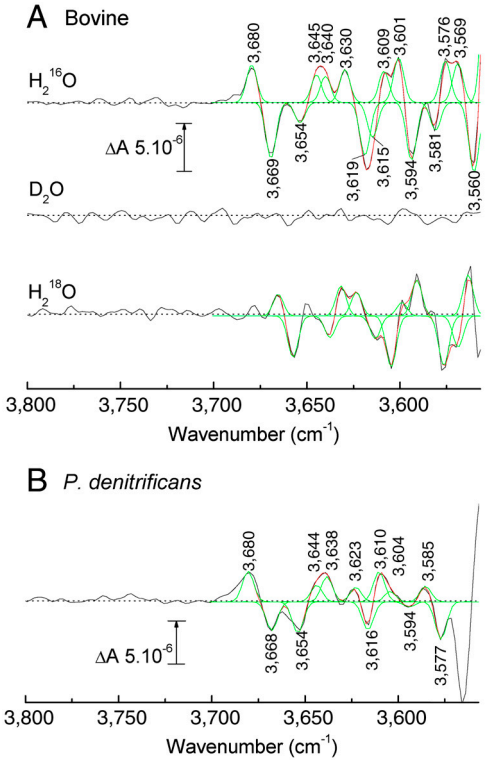

Fig. 2. Comparison of light-induced CO-photolysis transmission FTIR difference spectra of fully reduced CcO-CO from bovine and *P. denitrificans* CcOs. (*A*) Bovine CcO: FTIR difference spectra (black traces) were recorded in $H_2{}^{16}O$ (top trace, average of 4,000 transitions), D_2O (middle trace, average of 984), and $H_2{}^{18}O$ (lower trace, average of 1,500) media. Data in $H_2{}^{16}O$ and $H_2{}^{18}O$ media were fitted with combinations of Gaussian components all with a fixed FWHM of 6 cm^{-1} (red traces; individual Gaussians shown in green). Fitted band frequencies are tabulated in Table S1; (*B*) *P. denitrificans* CcO: FTIR difference spectrum (black trace) in $H_2{}^{16}O$ at pH 8.5 (average of 1,400 transitions). Data were fitted with combinations of Gaussian components all with a fixed FWHM of 6 cm^{-1} (red traces; individual Gaussians shown in green).

the signals arose from alterations of weakly H-bonded water molecules in the C*c*O structure.

In order to assess the number of water molecules that might be involved, the difference spectrum in $H_2{}^{16}O$ was simulated with a set of Gaussian components, all fixed to a nominal bandwidth (FWHM) of 6 cm^{-1}, which is typical for such water species (31). A reasonable fit required eight positive and seven negative bands (Fig. 2*A*, green overlays), corresponding to at least eight waters that either contribute bandshifts or positive signals. Three of these positives had similar frequencies to the three positive bands observed in the reduced *minus* oxidized difference spectrum (Fig. 1*A*), as should be the case because the positives arise from the unligated reduced form of C*c*O in both types of spectra.

Comparison with a Bacterial Homologue. Fig. 2*B* shows an equivalent CO-photolysis difference spectrum (pH 8.5; $H_2{}^{16}O$ buffer) in the high-frequency range obtained with a bacterial (*P. denitrificans*) form of C*c*O (lower trace). The general pattern of signals is similar to the bovine data (Fig. 2*A*, top trace). At least seven positive and five negative Gaussian components could be fitted to the *P. denitrificans* data between 3,700 and 3,575 cm^{-1} (Fig. 2*B*, red and green overlays) suggesting that at least seven water molecules reorganize on ligand binding to the fully reduced C*c*O.

Structural and Mechanistic Considerations. Water molecules have been identified crystallographically in several internal regions of subunit I of both bovine mitochondrial and bacterial C*c*Os (Fig. 3). Around 10 waters are located "below" E242/E278 in the D channel, the majority of which are in similar positions in bovine and *P. denitrificans* C*c*Os, though extending closer to E278 in the latter. Both also have a cluster of bound waters "above" the heme a_3 close to the Mg^{2+}/Mn^{2+} ion, together with water between the heme *a* propionates; some of these might form part of an "exit" pathway for protons that are translocated via E242/278. In published structures of oxidized C*c*Os, only three waters associated with the K channel have been located, again in similar positions in bovine and *P. denitrificans* enzymes (Fig. 3). Further waters have been detected crystallographically in the H channel region (Fig. 3). However, this channel is not continuous in bacterial C*c*O structures and has less resolved water molecules.

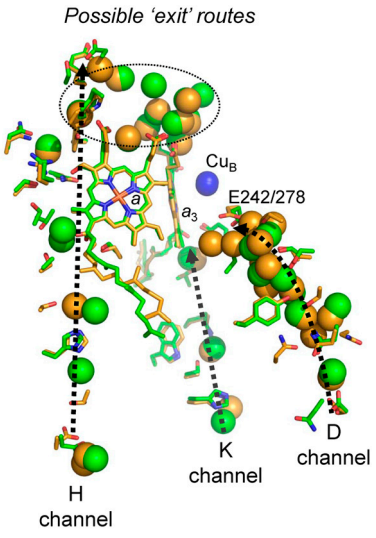

Fig. 3. Comparison of the hydrophilic channels and their associated water molecules in bovine and *P. denitrificans* C*c*Os. Crystal structures of subunit I of oxidized C*c*Os from bovine (PDB ID code 1V54 (26), green) and *P. denitrificans* (PDB ID code 3HB3 (13), orange) were aligned on their a_3 hemes. Amino acids and crystallographically resolved water molecules within the D, K, and H channels are displayed as spheres (green, bovine C*c*O; orange, *P. denitrificans* C*c*O). See text for details.

Roles for additional waters and structural mobility in these regions have been suggested. For example, there are gaps in protonic connectivity between E242/278 and the possible exit pathway and also between E242/278 and the binuclear center itself. It has been proposed that at least four crystallographically undetected, mobile water molecules in these regions might transiently reorganize during catalysis to provide gated protonic connectivity across these gaps (32, 33). In *Rb. sphaeroides* C*c*O, three additional waters appear between oxidized and reduced states in the region of the K channel closest to the BNC, whereas one is lost between E286 and the BNC (7). Data on bovine C*c*O indicate redox- and ligand-induced structural perturbations in the H channel region (4) and have led to the proposal that proton translocation might occur in bovine C*c*O via its H channel in a mechanism that is different to the D channel route in bacterial C*c*Os.

In bacteriorhodopsin, a prominent water signal has been reported in the 3,600–3,800 cm^{-1} region. This could be assigned to a water with a dangling OH group within a pentameric H-bonded structure formed with two other waters and adjacent amino acids (16). Identification of such waters in the available C*c*O structures is not presently feasible. The most likely location of the IR-detected waters described here is in the apparent gaps around E242/278 (34) and/or within the H channel region cavities (4) where water molecules might rearrange during catalysis to form transient gated proton pathways. Their weaker binding and more flexible conformations could prevent their being detected in present X-ray crystal structures. Observation of the water IR signatures during controlled redox potentiometry or conversion between intermediates, together with specific point mutations in the putative proton channels, provide a direct means to locate them and, therefore, to establish the proposed roles of these channels in the proton/electron coupling mechanism in different C*c*Os.

Concluding Remarks

These data show definitively that weakly H-bonded water molecules within the bovine C*c*O structure undergo structural perturbations in response to ligand (CO) changes at the binuclear center and to redox changes of the redox cofactor(s). Such structured water changes, working in concert with alterations of protonatable amino acids in one or more of the putative H, D, and K channels, are likely to be central to the C*c*O proton/electron coupling mechanism. The making and breaking of H bonds in water chains would provide the basis for formation of transient proton pathways and controlled gating during catalysis. It is noteworthy that the pattern of water changes observed are quite similar in both bovine mitochondrial and bacterial (*P. denitrificans*) forms of C*c*O. This suggests that a common proton coupling and gating mechanism is operative in both mitochondrial and bacterial systems.

Materials and Methods

Chemicals were purchased from Sigma-Aldrich and D_2O (D, 99.9%) and $H_2{}^{18}O$ (^{18}O, 97%) from Cambridge Isotope Laboratories, Inc. Nitrogen and carbon monoxide gases were purchased from BOC Ltd.

Cytochrome *c* Oxidase Preparations. Bovine cytochrome *c* oxidase was prepared from beef heart by a procedure (35) that yields "fast" enzyme with a characteristic Soret maximum at 424 nm. The final preparation was dissolved in 50 mM bicine, 0.1 mM potassium EDTA, 0.1% (wt/vol) Tween-80, pH 8.5, to a concentration of 150 μM, as quantitated from the dithionite-reduced minus oxidized optical difference spectrum using an extinction coefficient of $\Delta\epsilon_{606-621nm} = 25.7\ mM^{-1}\ cm^{-1}$ (36). Aliquots were stored at −80 °C until required. Wild-type *P. denitrificans* C*c*O was provided by Mårten Wikström (Institute of Biotechnology, University of Helsinki, Helsinki, Finland) and was prepared as in ref. 37.

FTIR Spectroscopy. Mid-IR spectra were recorded in attenuated total reflectance (ATR) or transmission mode with a Bruker IFS/66S FTIR spectrophot-

ometer fitted with a liquid nitrogen-cooled MCT-B detector at 4-cm^{-1} resolution, giving an accuracy of cited frequencies of ± 1 cm^{-1}. A narrow band filter (FWHM 4,020–3,620 cm^{-1}, Northumbria Optical Coatings Ltd.) was used to isolate the high-frequency region in order to increase signal/noise.

Electrochemically-Induced ATR-FTIR Redox Difference Spectra. CcO (1.5 nmol) was diluted in 2 mL of 50 mM KPi pH 8.5 + 0.1% (wt/vol) cholate and pelleted by ultracentrifugation at 300,000 × *g*, 4 °C, for 1 h. The process was repeated a second time with 50 mM KPi pH 8.5 and 30 min ultracentrifugation, and a third time with 1 mM KPi pH 8.5 and 15 min ultracentrifugation. The protein pellet was resuspended with 80 μL of 1 mM KPi pH 8.5 and aliquoted in 10-μL samples. These ATR-ready samples were flash-frozen in liquid nitrogen and stored and −80 °C until required. For each ATR-FTIR experiment, an ATR-ready sample was placed on a silicon prism (3-mm diameter, 3-bounce, SensIR Europe), dried under a nitrogen flow, and finally rewetted with the buffer of the experiment. Typically, such samples had an amide II band ΔA at 1,550 cm^{-1} of ≈0.14. An ATR-FTIR compatible cell with a platinum mesh working electrode was assembled on top of the sample layer. It was connected via a Vycor frit to platinum sheet counter and Ag/AgCl reference electrodes (38). The chamber was filled with a freshly prepared mediator solution and the sample was allowed to equilibrate for 1 h before starting any redox experiment. Buffer alone was placed in the reference/counter electrode chamber. Reduced *minus* oxidized spectra were induced electrochemically in 100 mM bicine at pH 8.5, containing 500 μM potassium ferricyanide and 50 μM benzyl viologen as redox mediators. Working electrode potentials (versus the standard hydrogen electrode) were +500 mV for oxidation and −400 mV for reduction. IR difference spectra were measured by recording a background spectrum (1,000 interferograms) at one potential, then switching to the second potential and recording a sample spectrum (1,000 interferograms) after 12-min equilibration. Redox cycles were repeated 452 times on three different samples and reductive and oxidative spectra were averaged to produce the redox spectra shown. Control spectra were regularly recorded over the full mid-IR spectral range in order to assess the quality and stability of the sample during data acquisition.

CO-Photolysis Difference Spectra by Transmission FTIR Spectroscopy. CcO (2 nmol) was reduced with 0.1 M Na dithionite in 0.1 M bicine pH 8.5 and left to equilibrate on ice for 30 min. The sample was then reoxidized and rinsed by repeated dilution/reconcentration in 10 mM bicine at pH 8.5 and 4 °C using ultrafiltration (Vivaspin, 30 kDa cutoff). The final concentrated protein sample (*ca.* 10 μL) was placed on a CaF_2 window, mixed with 1 μL of CO-saturated 0.2 M Na dithionite in 1 M bicine pH 8.5, and exposed to a stream of H_2O-saturated CO for 1 min, before placing a second window on top and sealing with silicon vacuum grease. Optimal samples had a ΔA of amide I + water at 1,650 cm^{-1} of ≈0.8 and of amide II at 1,550 cm^{-1} of ≈0.3. Actinic light was provided by a 250-W quartz-iodine lamp, filtered with glass, water, and a BG39 cutoff filter, and delivered to the sample via a light pipe. "Light *minus* dark *minus* dark" spectra were recorded at 277 K as follows (28): 100 interferograms were averaged to provide an initial dark baseline, after which the light was switched on and a sample spectrum (100 interferograms) recorded after 1 s. Finally, the light was switched off, and the recording was repeated after 1 s dark relaxation in order to provide an estimate of sample baseline drift. Light/dark cycles were repeated up to 4,000 times on three different samples and signal averaged to produce the data shown. Spectra in the mid-IR region were periodically checked during data acquisition to assess sample quality and stability.

D_2O and $H_2{}^{18}O$ Samples Preparation. Bovine CcO (2 nmol) was washed by dilution/reconcentration with 10 volumes of 10 mM bicine at pD/pH 8.5 in D_2O or $H_2{}^{18}O$ (39), using ultrafiltration (Vivaspin, 30 kDa cutoff). The sample was then diluted 10-fold in 10 mM bicine at pD/pH 8.5 containing 12 μM Tween-80, 5 mM Na ascorbate and 10 μM hexamine ruthenium (II) chloride, and incubated overnight at 4 °C. The sample was then diluted 3-fold in D_2O or $H_2{}^{18}O$, pelleted by ultracentrifugation at 300,000 × *g* for 1 h at 4 °C, and finally resuspended in 10 mM bicine containing 12 μM Tween-80 at pD/pH 8.5. The CcO-CO sample for transmission measurements was then handled as described above, but with D_2O or $H_2{}^{18}O$ buffers at pD/pH 8.5 and with a CO stream saturated with D_2O or $H_2{}^{18}O$ vapor.

ACKNOWLEDGMENTS. We are grateful to Prof. Mårten Wikström (Institute of Biotechnology, University of Helsinki, Helsinki, Finland) for his gift of the *P. denitrificans* CcO and to Mr. Santiago Garcia for specialist electronic and mechanical support. This work was funded by the British Biotechnology and Biological Sciences Research Council (Research Grant BB/H000097/1).

1. Rich PR, Maréchal A (2010) The mitochondrial respiratory chain. *Essays Biochem* 27:1–23.
2. Kaila VRI, Verkhovsky MI, Wikström M (2010) Proton-coupled electron transfer in cytochrome oxidase. *Chem Rev* 110:7062–7081.
3. Tsukihara T, et al. (1996) The whole structure of the 13-subunit oxidized cytochrome *c* oxidase at 2.8 Å. *Science* 272:1136–1144.
4. Muramoto K, et al. (2010) Bovine cytochrome *c* oxidase structures enable O_2 reduction with minimization of reactive oxygens and provide a proton-pumping gate. *Proc Natl Acad Sci USA* 107:7740–7745.
5. Iwata S, Ostermeier C, Ludwig B, Michel H (1995) Structure at 2.8 Å resolution of cytochrome *c* oxidase from *Paracoccus denitrificans*. *Nature* 376:660–669.
6. Svensson-Ek M, et al. (2002) The X-ray crystal structures of wild-type and EQ(I-286) mutant cytochrome *c* oxidases from *Rhodobacter sphaeroides*. *J Mol Biol* 321:329–339.
7. Qin L, et al. (2009) Redox-dependent conformational changes in cytochrome *c* oxidase suggest a gating mechanism for proton uptake. *Biochemistry* 48:5121–5130.
8. Wikström M, Jasaitis A, Backgren C, Puustinen A, Verkhovsky MI (2000) The role of the D- and K-pathways of proton transfer in the function of the haem-copper oxidases. *Biochim Biophys Acta* 1459:514–520.
9. Michel H (1999) Proton pumping by cytochrome *c* oxidase. *Nature* 402:602–603.
10. Shimokata K, et al. (2007) The proton pumping pathway of bovine heart cytochrome *c* oxidase. *Proc Natl Acad Sci USA* 104:4200–4205.
11. Pfitzner U, et al. (1998) Cytochrome *c* oxidase (heme aa_3) from *Paracoccus denitrificans*: Analysis of mutations in putative proton channels of subunit I. *J Bioenerg Biomembr* 30:89–97.
12. Lee H-M, et al. (2000) Mutations in the putative H-channel in the cytochrome *c* oxidase from *Rhodobacter sphaeroides* show that this channel is not important for proton conduction but reveal modulation of the properties of heme *a*. *Biochemistry* 39:2989–2996.
13. Koepke J, et al. (2009) High resolution crystal structure of *Paracoccus denitrificans* cytochrome *c* oxidase: New insights into the active site and the proton transfer pathways. *Biochim Biophys Acta* 1787:635–645.
14. Wikström M, Verkhovsky MI, Hummer G (2003) Water-gated mechanism of proton translocation by cytochrome *c* oxidase. *Biochim Biophys Acta* 1604:61–65.
15. Kandori H (2000) Role of internal water molecules in bacteriorhodopsin. *Biochim Biophys Acta* 1460:177–191.
16. Garczarek F, Gerwert K (2006) Functional waters in intraprotein proton transfer monitored by FTIR difference spectroscopy. *Nature* 439:109–112.
17. Noguchi T, Sugiura M (2002) FTIR detection of water reactions during the flash-induced S-state cycle of the photosynthetic water-oxidizing complex. *Biochemistry* 41:15706–15712.
18. Rozenberg M, Loewenschuss A, Marcus Y (2000) An empirical correlation between stretching vibration redshift and hydrogen bond length. *Phys Chem Chem Phys* 2:2699–2702.
19. Headrick JM, et al. (2005) The structure of protonated water clusters. *Science* 308:1765–1769.
20. Rich PR, Breton J (2002) Attenuated total reflection Fourier transform infrared studies of redox changes in bovine cytochrome *c* oxidase: Resolution of the redox Fourier transform infrared difference spectrum of heme a_3. *Biochemistry* 41:967–973.
21. Okuno D, Iwase T, Shinzawa-Itoh K, Yoshikawa S, Kitagawa T (2003) FTIR detection of protonation/deprotonation of key carboxyl side chains caused by redox change of the CuA-heme *a* moiety and ligand dissociation from the heme a_3-Cu_B center of bovine heart cytochrome *c* oxidase. *J Am Chem Soc* 125:7209–7218.
22. Nyquist RM, et al. (2001) Perfusion-induced redox differences in cytochrome *c* oxidase: ATR/FT-IR spectroscopy. *FEBS Lett* 505:63–67.
23. Iwaki M, Puustinen A, Wikström M, Rich PR (2003) ATR-FTIR spectroscopy of the P_M and F intermediates of bovine and *Paracoccus denitrificans* cytochrome *c* oxidase. *Biochemistry* 42:8809–8817.
24. Lübben M, Gerwert K (1996) Redox FTIR difference spectroscopy using caged electrons reveals contributions of carboxyl groups to the catalytic mechanism of haem-copper oxidases. *FEBS Lett* 397:303–307.
25. Rich PR, Maréchal A (2008) Carboxyl group functions in the heme-copper oxidases: Information from mid-IR vibrational spectroscopy. *Biochim Biophys Acta* 1777:912–918.
26. Tsukihara T, et al. (2003) The low-spin heme of cytochrome *c* oxidase as the driving element of the proton-pumping process. *Proc Natl Acad Sci USA* 100:15304–15309.
27. Gorbikova EA, Belevich NP, Wikström M, Verkhovsky MI (2007) Protolytic reactions on reduction of cytochrome *c* oxidase studied by ATR-FTIR spectroscopy. *Biochemistry* 46:4177–4183.
28. Rich PR, Breton J (2001) FTIR studies of the CO and cyanide compounds of fully reduced bovine cytochrome *c* oxidase. *Biochemistry* 40:6441–6449.
29. Rost B, et al. (1999) Time-resolved FT-IR studies on the CO adduct of *Paracoccus denitrificans* cytochrome *c* oxidase: Comparison of the fully reduced and the mixed valence form. *Biochemistry* 38:7565–7571.
30. Lappi SE, Smith B, Franzen F (2004) Infrared spectra of $H_2{}^{16}O$, $H_2{}^{18}O$ and D_2O in the liquid phase by single-pass attenuated total internal reflection spectroscopy. *Spectrochimica Acta A Mol Biomol Spectrosc* 60:2611–2619.
31. Takahashi R, Sugiura M, Noguchi T (2007) Water molecules coupled to the redox-active tyrosine Y_D in photosystem II as detected by FTIR spectroscopy. *Biochemistry* 46:14245–14249.
32. Tuukkanen A, Kaila VRI, Laakkonen L, Hummer G, Wikström MKF (2007) Dynamics of the glutamic acid 242 side chain in cytochrome *c* oxidase. *Biochim Biophys Acta* 1767:1102–1106.

33. Seibold SA, Mills DA, Ferguson-Miller S, Cukier RI (2005) Water chain formation and possible proton pumping routes in *Rhodobacter sphaeroides* cytochrome *c* oxidase: A molecular dynamics comparison of the wild type and R481K mutant. *Biochemistry* 44:10475–10485.
34. Kaila VRI, Verkhovsky MI, Hummer G, Wikstrom M (2008) Glutamic acid 242 is a valve in the proton pump of cytochrome *c* oxidase. *Proc Natl Acad Sci USA* 105:6255–6259.
35. Moody AJ, Cooper CE, Rich PR (1991) Characterisation of 'fast' and 'slow' forms of bovine heart cytochrome-*c* oxidase. *Biochim Biophys Acta* 1059:189–207.
36. Rich PR, Moody AJ (1997) *Bioelectrochemistry: Principles and Practice*, eds P Gräber and G Milazzo (Birkhäuser, Basel, Switzerland), pp 419–456.
37. Riistama S, Laakkonen L, Wikström M, Verkhovsky MI, Puustinen A (1999) The calcium binding site in cytochrome aa_3 from *Paracoccus denitrificans*. *Biochemistry* 38:10670–10677.
38. Rich PR, Iwaki M (2007) Methods to probe protein transitions with ATR infrared spectroscopy. *Mol Biosyst* 3:398–407.
39. Glasoe PK, Long FA (1960) Use of glass electrodes to measure acidities in deuterium oxide. *J Phys Chem* 64:188–190.